IMPROVING AND PREDICTING THE PETROPHYSICAL PARAMETERS OF THE RESERVOIRS USING MONTE CARLO SIMULATION AND STOCHASTIC ANALYSIS

Aref Lashin[*], Gamal Mosa[*] and Mohamed Abd El-Aal[**]

Geology Department, Faculty of Science, Benha University.
Mathematics Department, Faculty of Science, Benha University.
**Geology Department, Faculty of Education, Ain Shams University.*

تحسين و إستنتاج المعاملات البتروفيزيائية للخزانات بإستخدام المحاكاة بطريقة مونت كارلو و تحليل التغير الإحتمالي

الخلاصـــــة: تهتم هذه الدراسة بإستخدام نموذج يعتمد علي المحاكاة بالمونت كارلو وتحليل التغير الإحتمالي و يستند أساسا إلي أسس جيولوجية و ذلك لتحسين و لإستنتاج الخواص البتروفيزيائية للخزانات الحاملة للهيدروكربونات. هذا ويعتمد تحليل التغير الإحتمالي علي مجموعة مختلفة من دوال الكثافة الإحتمالية ومعامل المضاهاة والتباين والتباين المشترك لبيانات تسجيلات الآبار المستخدمة في الدراسة بالاضافه إلي التحليلات الإحصائية متعددة المتغيرات. قبل البدء في نظام المحاكاة تم إستخدام نوعين من الشروط (شروط ثابتة و أخري مرنة) و ذلك للإرشاد والتحكم في نموذج المحاكاة. ثم بعد ذلك تم إجراء المحاكاة و ذلك بتكرار المحاولة 100 مره لكل مستوي في الخزان و ذلك لحساب الخواص البتروفيزيائية الضرورية لدراسة وتقييم الخزان. هذا وقد تم تطبيق نموذج المحاكاة علي منطقتين مختلفتين (منطقة شمال شرق دلتا النيل البحرية وحقل رأس فنار). ففي منطقة شمال شرق دلتا النيل البحرية تم تطبيق النموذج لتحسين المعاملات البتروفيزيائية المقاسة للطبقات الحاملة للغاز وكذلك لتقليل الأخطاء الناتجة في التفسيرات نظرا لعدم دقة بعض الطرق الإحصائية المستخدمة في قياس بعض التسجيلات الكهربية مثل تسجيل إشعاع جاما و المسامية الظاهرية المحسوبة من تسجيل النيترون الثنائي علي سبيل المثال. كما تم إستخدام العديد من توزيعات المونت كارلو لحساب مختلف المعاملات اللازمة لتقييم الخزان وخاصة معاملات الطفلة وكذلك للتنبوء بالبارامترات البتروفيزيائية للآبار في المناطق التي تم التحقق من شرط الجوار الطوبو-جيولوجي فيها. أما في منطقة حقل رأس فنار تم إستخدام نموذج المحاكاة لحل مشكلة تخطي الحلقة الخاصة بالتسجيل الصوتي. وتعد مشكلة تخطي الحلقة من أبرز المشاكل في حقل رأس فنار المتعلقة بالخواص الصوتية لخزان النلليبور الكربوناتي. وقد وجد أن البارامترات البتروفيزيائية المستنتجة بإستخدام المحاكاة أكثر دقة و تمثيلا لخواص الخزان من تلك المستنتجة بإستخدام الطرق التقليدية لتسجيلات الآبار. و لذا يمكننا القول بأن هذا النموذج يمكن تطبيقه في المناطق الشبيهة ذات المعلومات القليلة أو قليلة الجودة و كذلك في المناطق الجديدة و ذلك للحصول علي أمثل تفسير للبيانات المتاحة كما يمكن إستخدام هذا النموذج لإستنتاج بعض الأجزاء المفقودة لتسجيلات بعض الآبار وكذلك للتنبؤ بالمعاملات البتروفيزيائية للآبار الإستكشافية الجديدة.

ABSTRACT: *In this study, Monte Carlo simulation and stochastic modelling analyses, in combination with geological-based concepts, are used to improve and predict the petrophysical parameters of the hydrocarbon-bearing reservoirs. The stochastic input is supplied in the form of probability density functions, correlation, and variance-covariance coefficients as determined from actual well logging data. The multivariate statistical analyses are used to produce correlated multivariate stochastic variables. Before going on the simulation model, two types of constraints (hard constraints and simulation constraints) are used to guide and control the simulation procedure. Monte Carlo simulation algorithm is then performed by running a 100 times iteration in front of each depth increment using correlated multivariate variables.*

The present simulation model is applied in two different case studies (Northeastern offshore Nile Delta and Ras Fanar field). In the offshore Nile Delta, the model is applied to improve the petrophysical parameters of the gas-bearing reservoirs. All logging data are simulated so as to, the uncertainty in the interpretations due to some errors like that in the statistics of gamma ray counting and in the estimation of apparent porosity from dual neutron log, are greatly reduced. Different Monte Carlo-based distributions are used to derive the different parameters necessary for reservoir evaluation especially those of shale. The model is used also to predict the petrophysical parameters of wells providing that a satisfactory topological/geological neighbourhood hard constraint is well developed in the area. In Ras Fanar field, the simulation algorithm is used to solve the cycle skipping problem which is another important and common problem concerning with sonic log due to the characteristic acoustic properties of the Nullipore carbonate reservoir. The simulated petrophysical parameters are found to be more realistic and representative for the actual petrophysical parameters of the reservoirs than those estimated using conventional logging analyses. So, this simulation model can be used not only as enhancement procedure in similar areas where the information is scarce or of bad quality and even in new areas to secure optimum use of the available data, but also as a predictive tool to predict the missed sections of logs and/ or to predict the petrophysical parameters of a new exploratory well.

1. INTRODUCTION

Computer simulation using Monte Carlo methods provides a powerful tool for the analysis of the parameters used in the volumetric studies, which is not possible using the traditional analytical approaches.

The origin of the modern Monte Carlo methods stems from work on the atomic bomb during the second world war when they were mainly used for numerical simulation of the neutron diffusion in fissile material, which is a probabilistic problem. Later on, it was realized that Monte Carlo methods could also be used

for deterministic problems (Sambridge and Mosegaard, 2002).

Monte Carlo is a random sampling method and requires a large sampling number N for accurate estimation. The algorithm relates and controls the uncertainty distributions of the individual parameters by a random number function (between 0 and 1) which performs numerous random iterations for each distribution. So, Monte Carlo simulation is used to solve certain stochastic (involving a random variable) problems where the passage of time plays no substantive role. Nowadays, it is widely used to solve certain statistical problems that are not analytically tractable. In geo-scientific applications, the method is used in many aspects such as reserve estimation and for prospect evaluation (de Groot et al. 1996).

Many authors dealt with applying the geostatistical stochastic modelling and simulation techniques in solving certain geological and petrophysical problems, of them the following are the most important; Bartlett (1966); Rubinstein (1981); Haldorsen and Chang (1986); Isaaks and Srivastava (1989); Strauss and Sadler (1989); Alabert and Massonnat (1990); Haldorsen and Damsleth (1990); Fogg et al. (1991); Law and Kelton (1991); Bortoli, et al. (1993); de Groot et al. (1993 and 1996); Molz and Boman (1993), Deutsch (2002), Pyrcz and Deutsch (2003); Pyrcz et al. (2005), ...etc.

2. MONTE CARLO SIMULATION AND RESERVOIR PARAMETERS

In conventional logging analyses, there are many difficulties concerning accurate estimation of the petrophysical properties of the reservoir of interest. In many cases, the anticipated outcomes depend on several input variables whose values may not be known exactly. Although, majority of logging data have to be corrected before going in the interpretations, still some uncertainties in the final calculations may arise. This can be argued in many cases to the methods by which some logs, especially the old ones, are recorded and finally presented. The mathematical procedure used in counting and presenting the gamma ray log and neutron porosity (far/near ratio) and the average method followed in calculating the interval transit time in case of the compensated sonic log, are two examples of the expected uncertainties which could further influence the final interpretations.

Another common problem, which if not treated carefully, may cause cumulative error in the calculations, is the choice of some important parameters like; the shale and matrix ones. As the complexity of the system to be interpreted increases, the conventional quantitative techniques used for reservoir analysis

become more and more unsuitable and uncertain. To deal with these problems, the actual well logging data can be analyzed by a stochastic simulation method, such as Monte Carlo simulation to improve the estimation of the properties of the reservoir of interest. The inputs are probability distributions, and the output of such stochastic methods is also given in terms of distributions.

2.1 Uncertainty in Logging Data

As mentioned earlier, there are many reasons for the uncertainty in logging measurements. Most of the expected errors are argued to the statistical methods which are followed while counting and converting certain logging data from form to another. The following are some examples of these errors:

Error Propagation in the Statistics of GR Counting (CPS to API)

The natural gamma ray can be run in both open and cased holes, either empty or fluid-filled. This log may be recorded in API units or counts per second, CPS. The nature of gamma ray emission is statistical and must be averaged over time (Hearst and Nelson, 1985). The detector stability and the length of time required to obtain a stable count rate depend upon the radioactivity of the target and efficiency of the detector. The primary calibration standard of gamma ray tools is the API units. So, when measured in CPS units, the gamma ray logs must be calibrated and converted to the API units.

Different statistical and probability distribution functions are used to model and calibrate the measured CPS radioactive count rate in a given time window (t). The most important parameter which affects the measurement, is the count rate error. Using the rules of propagation of error, the count rate error can be estimated as follows:

$$\sigma X = \sqrt{X} \quad \text{...(1)}$$

$$\sigma r = \frac{\sqrt{n}}{t} = \frac{\sqrt{X}}{t} \quad \text{...............................(2)}$$

$$\sigma G = \frac{200 * \sigma \Delta}{\Delta r^2} \quad \text{...............................(3)}$$

$$\sigma Av = \frac{\sigma API * \sigma X}{2} \quad \text{...............................(4)}$$

where:
X   is the number of counts per time window (t),
σX is the standard deviation,
σr is the count rate error,
t   is the time windows (t),
σG is the calibration gain standard deviation,
σAv is the count rate error standard deviation.

Taking the count rate error in consideration, the raw gamma ray count rate in CPS can be converted and calibrated to API units as follows:

$$GR\,(API) = \frac{200}{\Delta_r} GR\,(CPS) \quad\cdots\cdots\cdots\cdots\cdots\cdots\cdots\cdots\cdots(5)$$

$$GR\;fin\;(API) = GR\;(API) - \sigma\;Av \quad\ldots\ldots\ldots\ldots\ldots\ldots..(6)$$

where:

GR (CPS) is the gamma ray in count per second,
GR (API) is the gamma ray in API units,
Δ_r is the count rate difference.

The previous statistical calibration is so complicated and in many cases leads to an expected effective error in the raw values of the converted API gamma ray units. So all conventional well log analyses which make use of gamma ray log will have some uncertainties and cause some errors in the final results, the effect which could be eliminated if a suitable Monte Carlo distribution is used instead. It is worth to mention here, that some environmental corrections of gamma ray log such as correction of gamma ray log for bore hole condition and mud barite (GR-1 and GR-2 charts, Schlumberger Charts 1991) are based mainly on the Monte Carlo simulation technique.

NPHI Porosity Estimation Form Dual Neutron (Ratio-to-Porosity Transform)

Porosity is one of the most important petrophysical properties, which must be carefully determined for good evaluation and assessment of the reservoir of interest. Many logging tools are used for accurate porosity estimation, among them is the dual neutron tool which is considered one of the most recent and important tools. It employs a chemical source of neutrons and two thermal neutron detectors. The actual measurement consists of the calibrated ratio of the far-detector to near-detector count rates (Mod-8 ratio to porosity transform).

The far/near count ratio is related to the hydrogen content of the formation. When hydrogen is associated with liquid-filled pore space, this ratio can be used to determine the classic NPHI porosity. The following is the ratio-to-porosity transform which is used for fraction porosity estimation:

$$Ratio \;\; = \frac{Far\;detector\;(CPS)}{Near\;\;detector\;(CPS)} \quad\cdots\cdots\cdots\cdots\cdots..(7)$$

Having the porosity ratio, the environmentally uncorrected apparent limestone porosity can be estimated using the special user function for the dual neutron probe as follows:

$$TMP3 \; = (TMP2)^2 \quad\ldots\ldots\ldots\ldots\ldots\ldots\ldots\ldots\ldots..(8)$$

$$TMP4 \; = (TMP2)^3 \ldots\ldots\ldots\ldots..\ldots\ldots..\ldots\ldots\ldots.(9)$$

TMP5 = (0.1080258/ TMP4) - (0.25482/ TMP3) + (4.779079/ TMP2) - 9.517288 ……………......(10)

TMP6 = (0.1149102/ TMP4) - (0.25482/ TMP3) + (4.85726/ TMP2) - 8.734154 ……………..…......(11)

TMP7 = (TMP5 - TMP6) …..………………........(12)

TMP8 = TMP6 – (TMP7 * B.S) ..………….…........(13)

NPHI = (TMP7 * TMP1) + TMP8 ……...……….....(14)

where:

NPHI   is the apparent limestone porosity,
TMP1   is the caliper log readings (mm),
TMP2   is the far/near ratio (CPS),
TMP7 and TMP8 are the slope and intercept of the calibrated porosities at borehole diameters of 214 mm and 150 mm, respectively.

The above mentioned statistical technique has the advantage of effectively compensating for the variations in borehole and formation salinity from one hand and minimizing the effects of changes in borehole size (caliper corrected) from the other hand. But still some difficulties and exaggerated errors in the final estimated apparent porosity due to the normal regression analysis used for solving the equations.

2.2 Simulation Algorithm and Model Structure

Monte Carlo simulation can be used for a variety of different petrophysical problems, which are not so easy to be treated by the traditional logging analyses. The procedure of Monte Carlo simulation depends on numerous probabilities for certain samples to approximate the solution of any mathematical or physical problem in a statistical way. The successful simulation model must be realistic representative of the subsurface geological feature (reservoir) to be studied. So the input of the simulation algorithm is a combination of stochastic correlated parameters and geological-based information controlled by certain constraints.

To deal with the uncertainty, some rules are used in the reservoir simulation, the first are the petrophysical-related ones which governorate the whole simulation framework, while the others are stochastic realizations which can be re-evaluated and redrawn, until satisfactory result is achieved. The stochastic inputs are supplied in the form of probability density functions (pdf's) variance-covariance and correlation coefficients matrices as determined from actual well logging data.

Constraints

Before going on the simulation model, we have to define some constraints, which will guide and control the simulation procedure. There are two types of

constraints, hard constraints and simulation constraints. The hard constraints, as used in this study, include number of probability density functions (pdf's) for the different studied zones, in addition to rules which keep the main petrophysical characteristics of different zones (ρb - ϕN log responses in front of gas zones) and finally certain topo-geological relationship between simulated wells in the area. At any stage of the simulation the stochastic variables are evaluated against the hard constraints. If any hard constraint is not satisfied, then the variables are redrawn again and so on.

The simulation constraints, on the other hand, include petrophysical-related rules such as; shale and matrix parameters, lithology type, and the number of different zones (entities) used in the study and their relative thicknesses.

Correlated Stochastic Variables

In this study multiple geostatistical techniques are applied to generate correlated distributions of the reservoir rock parameters. For example, if we have three correlated logging parameters or variables (X1, X2 and X3), that satisfy the relation:

$$E\left[X_1 \mid X_2 = x_2 \right] \text{ is linear in } x_2 \quad \ldots\ldots\ldots\ldots\ldots\ldots(15)$$

$$E\left[X_1 \mid X_3 = x_3 \right] \text{ is linear in } x_3 \quad \ldots\ldots\ldots\ldots\ldots\ldots(16)$$

Then it will be possible to get correlated stochastic variables of the logging data by constructing two types of matrices (correlation and variance-covariance). By definition, the forms of these two matrices can be written as follows:

Correlation Matrix :

$$\begin{array}{c} \\ X_1 \\ X_2 \\ X_3 \end{array} \begin{array}{ccc} X_1 & X_2 & X_3 \end{array} \\ \begin{pmatrix} \rho_{11} & \rho_{12} & \rho_{13} \\ \rho_{21} & \rho_{22} & \rho_{23} \\ \rho_{31} & \rho_{32} & \rho_{33} \end{pmatrix} \ldots\ldots\ldots\ldots\ldots\ldots\ldots\ldots(17)$$

Variance-Covariance Matrix:

$$\begin{array}{c} \\ X_1 \\ X_2 \\ X_3 \end{array} \begin{array}{ccc} X_1 & X_2 & X_3 \end{array} \\ \begin{pmatrix} \sigma_{11} & \sigma_{12} & \sigma_{13} \\ \sigma_{21} & \sigma_{22} & \sigma_{23} \\ \sigma_{31} & \sigma_{32} & \sigma_{33} \end{pmatrix} \ldots\ldots\ldots\ldots\ldots\ldots\ldots(18)$$

Where the correlation (ρ) and covariance ($\sigma_{x1,x2}$) can be identified as follows:

Corr. (ρ) = $\sigma_{x1,x2 / (\sigma_{x1} * \sigma_{x2})}$ $\ldots\ldots\ldots\ldots\ldots\ldots..(19)$

Cov. $(\sigma_{x1,x2})$ = E $[(x_1 - \mu_{x1}) (x_2 - \mu_{x2})]$$\ldots\ldots\ldots(20)$

Correlated Multivariate Variables

The general form of the multivariate variables (*MVN*) is:

$$X \sim M V N \left(\mu , \sigma \right) \ldots\ldots\ldots\ldots\ldots\ldots\ldots(21)$$

So the conditional distribution of X1 which gives a realization *x2* of X2 is *MVN* with expectation:

$$\hat{\mu}_1 = \mu_1 + \sigma_{12}\sigma_{22}^{-1} \left(x_2 - \mu_2 \right) \ldots\ldots\ldots\ldots\ldots(22)$$

$$\hat{\sigma}_{11} = \sigma_{11} - \sigma_{12}\sigma_{22}^{-1}\sigma_{21} \ldots\ldots\ldots\ldots\ldots\ldots(23)$$

So, if we have 5 variables or logs, namely; ρb (x1), ϕN (x2), ΔT(x3), GR (x4) and Rt (x5), these variables can be correlated together in multivariate arrangement as follows:

$$\hat{\mu}_3 = \mu_3 + \left[\sigma_{31}\sigma_{32}\right] \begin{pmatrix} \sigma_{11} & \sigma_{12} \\ \sigma_{12} & \sigma_{22} \end{pmatrix}^{-1} \begin{pmatrix} x_1 & - & \mu_1 \\ & & \\ x_2 & - & \mu_2 \end{pmatrix} \ldots.(24)$$

$$\hat{\sigma}_3^2 = \sigma_3^2 - \left[\sigma_{31}\sigma_{32}\right] \begin{pmatrix} \sigma_{11} & \sigma_{12} \\ \sigma_{12} & \sigma_{22} \end{pmatrix}^{-1} \begin{bmatrix} \sigma_{31} \\ \sigma_{32} \end{bmatrix} \ldots\ldots\ldots\ldots(25)$$

Where $\hat{\mu}_3$ and $\hat{\sigma}_3$ are stochastically derived parameters of ΔT log (x3), which could be further redrawn (simulated) using a suitable Monte Carlo distribution.

APPLICATIONS

The present simulation model is applied in two different areas (Fig. 1); in the offshore Nile Delta and Ras Fanar field; as an attempt to predict and enhance the estimation of the petrophysical parameters of the hydrocarbon-bearing reservoirs in these areas.

Figure (1): Map showing the location of the study areas.

In the offshore Nile Delta, the model is applied to improve and predict the petrophysical parameters of the gas-bearing reservoirs. While in Ras Fanar field, the simulation algorithm is used mainly to solve the cycle skipping problem concerning with sonic log which is common phenomenon in this field due to the acoustic properties of the Nullipore carbonate reservoir.

CASE STUDY 1: OFF SHORE NILE DELTA

The Northeastern offshore Nile Delta (Figs. 1 and 7) is one of the promised areas for gas exploration in Egypt. The sedimentary succession of this area consists of interbedded clastics (sand and shale). Several gas discoveries have been made in this area since the mid of 1993. Most of the gas-bearing sand anomalies are entrapped stratigraphically in sediments of Late Pliocene to Early Pleistocene in age. The main Plio-Pleistocene hydrocarbon entrapment style in this area is related to the channelized meandering system in part and to the hanging wall rollover anticlinal closures of the listric faults in the other.

PROBABILITY DENSITY FUNCTIONS (PDF'S)

A number of probability density functions (pfd's) are constructed for a number of wells in the area. The study sections (Pliocene gas-bearing formations) are classified in terms of shale content, into number of clean sand and shale entities or zones.

Then, different types of pfd's are constructed for each of these zones separately. These functions are very important as it determine the type of the distribution and the best guess of the parameters which will be further used in simulating certain petrophysical property. Figure 2 shows an example of the constructed probability density functions (pfd's) for the gas-bearing sand and shale zones in Darfeel-7 well.

The figure gives best chance or highest probabilities of 0.56 and 0.71 with mid points of 45.30 and 66.10 for the gamma ray log in the gas sand and shale zones, respectively.

DISTRIBUTIONS FOR SHALE PARAMETERS DETERMINATION

Finding the different parameters of the reservoir under study, including the shale parameters, is very important step before going in any analytical process. The good picking of these parameters, the more accurate will be the final interpretations. Since the gas-bearing sand anomalies are embedded mainly in different shale sediments, and are encountered at different depth levels with different geological ages, this necessitates careful choosing of the different shale parameters, especially for the shale beds which have different environments of deposition. In traditional well logging analysis these parameters are usually selected using many qualitative and quantitative techniques with considerable error ratio.
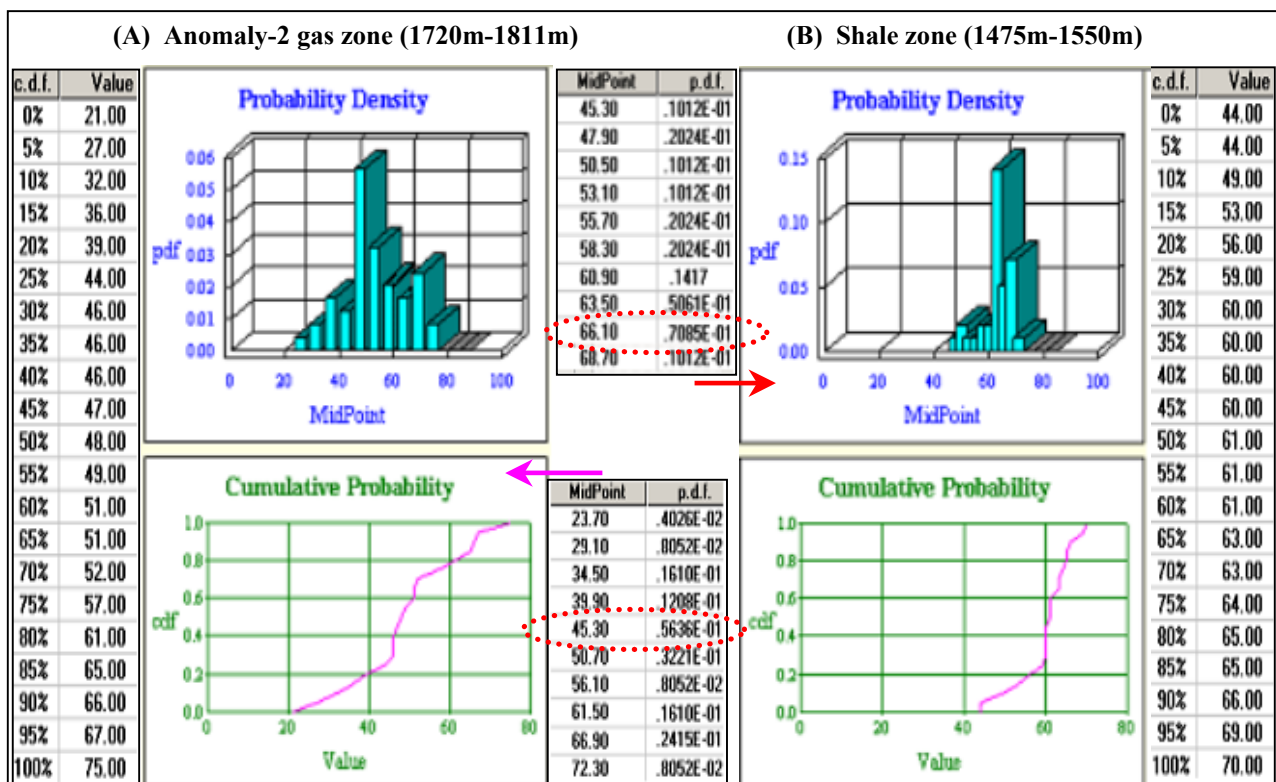

Figure (2): Gamma ray probability density functions (pdf's) of the gas sand and shale zones, Darfeel-7 well.

In this study, and by using iteration of 100 times in front of each depth increment of the studied zones, shale parameters are picked through random distributions based on Monte Carlo simulation. Table (1) shows the different statistical parameters of the available logging data of two selected wells (Darfeel-1 and Darfeel-2) used as examples in the offshore Nile Delta area. These parameters will be utilized, with some limitations, as key inputs for any random distribution which will be used for acquiring the new simulated shale parameters. Very high variance and Std. Dev. values are recognized for the resistivity log in both wells due to the presence of a number of gas-bearing anomalies with much higher recorded resistivity, especially in Darfeel-1 well.

Based on the probability density functions of the shale zones in the study area, the normal and lognormal distributions (Fig. 3) are found the most appropriate for running the simulation process. The general forms of these two distributions are as follows:

Normal Distribution:

$$f(x) = \frac{1}{\sqrt{2\pi b^2}} \exp[-\frac{(x-a)^2}{2b^2}] \quad \dots\dots\dots\dots\dots\dots(26)$$

Lognormal Distribution:

$$f(x) = \frac{1}{x\sqrt{2\pi b^2}} \exp[-\frac{(\ell nx - a)^2}{2b^2}]$$
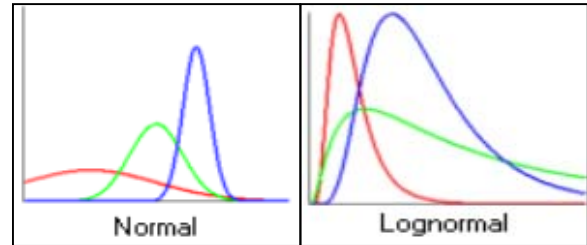$$\dots\dots\dots\dots\dots\dots(27)$$

Figure (3): Normal and lognormal distributions.

Table (2) summarizes the different estimated and simulated shale parameters using Monte Carlo simulation for Darfeel-1and Darfeel-2 wells.

Table (1): The average, variance and standard deviation parameters of the main logs in Darfeel-1 and Darfeel-2 wells.

Well	Param.	ΔT	ρb	ϕN	Rt	GR
Darfeel-1	μ	134.67	2.110	35.75	9.00	65.00
	σ^2	193.21	0.009	59.52	949.25	81.99
	St.Dev.	13.90	0.098	7.71	30.81	9.05
Darfeel-2	μ	132.68	2.150	41.21	4.02	61.00
	σ^2	256.32	0.011	57.30	59.91	74.13
	St.Dev.	16.01	0.082	7.57	7.74	8.61

Table (2): Shale parameters estimated by normal logging and simulation methods, Darfeel-1 and Darfeel-2 wells.

Well	Model	Param.	ΔT_{sh}	ρb_{sh}	ϕN_{sh}	Rt_{sh}	GR_{min}	GR_{max}
Darfeel-1	**Logging**	Log_{sh}	138.04	2.132	40.02	0.92	42.12	72.13
	Monte Carlo Sim.	μ	139.82	2.141	41.9	0.89	40.36	75.94
		σ^2	313.29	0.004	69.14	0.05	14.98	27.77
		St.Dev.	17.70	0.062	8.315	0.23	3.87	5.27
		Log_{sh}	140.53	2.122	42.46	0.96	39.93	75.29
Darfeel-2	**Logging**	Log_{sh}	142.11	2.114	41.05	0.95	41.21	65.24
	Monte Carlo Sim.	μ	139.62	2.134	43.32	0.91	38.44	68.04
		σ^2	25.20	0.002	14.29	0.07	7.40	14.82
		St.Dev.	5.02	0.048	3.78	0.26	2.72	3.85
		Log_{sh}	141.54	2.126	41.7	0.88	40.25	67.68

IMPROVING THE PETROPHYSICAL PARAMETERS

After preparing the probability density functions and choosing the suitable distribution for each petrophysical parameter, then logging data can be randomly iterated and another new stochastically derived parameters can be obtained. By making iteration of 100 times at each depth level for each petrophysical parameter to be deduced and by taking the best chance (most likely), then we will have much improved and stochastically new correlated petrophysical parameters.

The above procedure can be used to improve the estimation of the petrophysical parameters from one hand and to minimize the error ratio in the final interpretations to large extent, from the other hand. Figure (4) shows an example of complete petrophysical analysis of Darfeel-1 well based on Monte Carlo simulation.
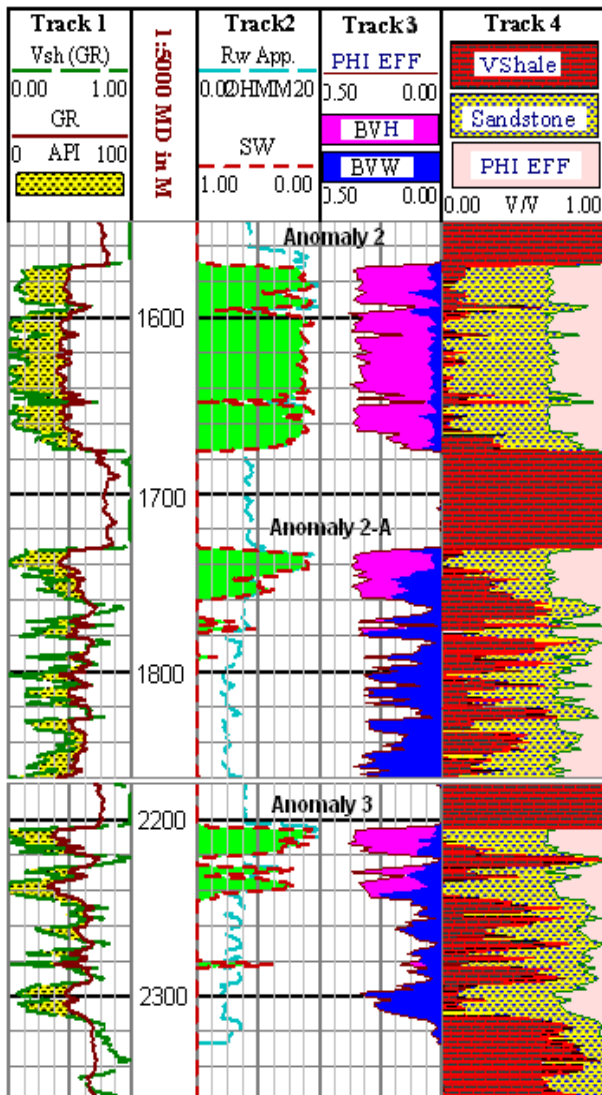

Figure (4): Petrophysical analysis of the Darfeel-1 well based on Monte Carlo simulation.

Three gas-bearing sand levels are well detected (anomalies 2, 2-A and 3) at different depth levels, associated with high apparent water resistivity. The petrophysical analysis of these levels show high effective porosity (> 25%), high gas saturation (>50%) and low shale volume. Table (3) exhibits the normalized values for the main petrophysical parameters of the detected gas-bearing anomalies using normal logging analyses and simulation method. An effective range of differences can be observed between the results of both methods.

Table (3): Average petrophysical parameters of the gas-bearing anomalies in Darfeel-1 well.

Method	Zone	Vsh	Sw	ϕeff
Monte Carlo Sim.	Anomaly 2	0.12	0.20	0.30
	Anomaly 2-A	0.37	0.57	0.24
	Anomaly 3	0.19	0.35	0.28
Normal Logging	Anomaly 2	0.18	0.28	0.25
	Anomaly 2-A	0.30	0.64	0.21
	Anomaly 3	0.24	0.39	0.24

Another application of the simulation technique, is to redraw some petrophysical parameters which are not commonly used in logging analyses due to the uncertainty associated in the final interpretations such as; some single and double porosity (Sonic, Neutron-Sonic, Gamma-Sonic,…etc.) and shale volume indicators (Resistivity, Neutron,... etc.). In this respect, shale volume is used as example to demonstrate the expected petrophysical improvements and differences, which may arise upon applying the simulation technique. Nouras-1 well (Fig. 7) is selected for this purpose and shale volumes are estimated using gamma ray, neutron and resistivity logs. Usually gamma ray log is the best for this process; meanwhile neutron and resistivity logs, in most cases, give very bad interpretations. In this example, GR log is used as reference log, which means that this log is corrected and randomly iterated before being used by both methods. The following are the correlation and variance-covariance matrices for shale volume estimated using these single log indicators:

Correlation Matrix (Logging):

$$
\begin{array}{c}
\\
\text{Vsh}_{GR} \\
\text{Vsh}_{Neut} \\
\text{Vsh}_{Rt}
\end{array}
\begin{array}{ccc}
\text{Vsh}_{GR} & \text{Vsh}_{Neut} & \text{Vsh}_{Rt} \\
\left(1.00 \right. & 0.621 & \left. 0.419 \right) \\
\left(0.621 \right. & 1.00 & \left. 0.225 \right) \\
\left(0.419 \right. & 0.225 & \left. 1.00 \right)
\end{array}
$$

Variance-Covariance Matrix (Logging):

$$
\begin{array}{c}
\\
\text{Vsh}_{GR} \\
\text{Vsh}_{Neut} \\
\text{Vsh}_{Rt}
\end{array}
\begin{array}{ccc}
\text{Vsh}_{GR} & \text{Vsh}_{Neut} & \text{Vsh}_{Rt} \\
\left(0.1038 \right. & 0.0374 & \left. 0.0616 \right) \\
\left(0.0374 \right. & 0.0353 & \left. 0.0192 \right) \\
\left(0.0616 \right. & 0.0192 & \left. 0.2097 \right)
\end{array}
$$

One can easily note that, the correlation between the different shale volumes is not so good especially between neutron-resistivity logs (ρ =22%) and gamma ray-resistivity logs (ρ =41%). On the other hand, the correlation matrix for the different simulated shale volumes shows much better improvements. In general, very good correlation (ρ >72%) is recognized between the different simulated volumes.

Correlation Matrix (MC Sim.):

$$
\begin{array}{c}
\\
\text{VshGR} \\
\text{VshNeut} \\
\text{VshRt}
\end{array}
\begin{array}{ccc}
\text{VshGR} & \text{VshNeut} & \text{VshRt} \\
\left(1.00 \right. & 0.801 & 0.724 \\
0.801 & 1.00 & 0.863 \\
\left. 0.724 \right. & 0.863 & 1.00
\end{array}
$$

Variance-Covariance Matrix (MC Sim.):

$$
\begin{array}{c}
\\
\text{VshGR} \\
\text{VshNeut} \\
\text{VshRt}
\end{array}
\begin{array}{ccc}
\text{VshGR} & \text{VshNeut} & \text{VshRt} \\
\left(0.1041 \right. & 0.0595 & 0.0482 \\
0.0595 & 0.0540 & 0.0413 \\
\left. 0.0482 \right. & 0.0413 & 0.0430
\end{array}
$$

.

Further more, the variance-covariance matrix of the simulated data exhibits very good range (0.0413-0.1041), which is much correlated and closer than that provided by normal logging analyses (0.0192-0.02097). Table (4) shows an example of the statistical analysis of the different shale volumes of Nouras-1 well. While the average estimated shale volumes exhibit wide range (53% from GR log, to 68% from Rt log), the simulated data show close improved range in the order of 53% to 60%.

Table (4): Statistical analysis of different shale volumes, Nouras-1 well.

Method	Param.	μ	σ^2	St. Dev.
Normal Logging	Vsh GR	0.536	0.104	0.322
	Vsh Neut.	0.634	0.035	0.187
	Vsh Rt	0.687	0.209	0.457
Monte Carlo Sim.	Vsh GR	0.536	0.104	0.322
	Vsh Neut.	0.601	0.054	0.231
	Vsh Rt	0.597	0.043	0.207

Figure (5) shows the shale volume analog for the different shale curves estimated by the logging (Track 3) and simulation (Track 5) methods.
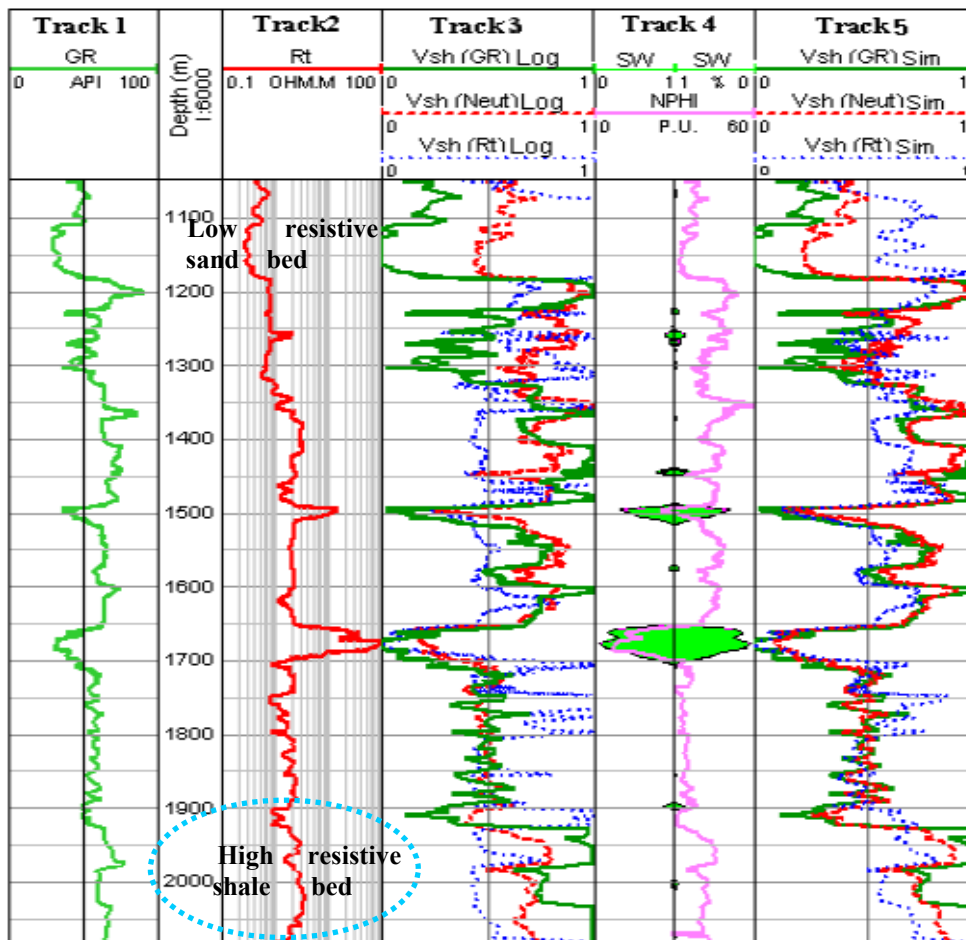

Figure (5): Shale volume analog of Nouras-1 well.

Regarding track 3, very bad matching is observed between resistivity-derived shale volume and other shale volumes estimated from neutron and gamma ray logs allover the entire section of the well and between all of them especially in the upper and lower parts of the study section. This is urged to the presence of low resistive clean sand bed in the upper part of the section (1108m-1185m) which leads to high exaggerated shale volume as compared with other volumes derived from neutron and gamma ray logs. Another reason is the presence of high resistive shale bed in the lower part of the section (1940m-2045m), which could be interpreted by the resistivity log as clean bed with much reduced shale volume. Track 5 on the hand, shows the simulated shale volumes. The matching between the resistivity-derived shale volume and other estimated shale volumes (neutron and gamma ray) is remarkably improved in the upper and lower parts of the study section and between all of them allover the entire section of the well, in general.

To clarify the differences between the two methods in a more detailed statistical way, frequency and percent analyses are carried out upon the different concluded shale volumes. Figure (6) shows the frequency crossplots of both log-derived and simulated data. The circular selections exhibit the low and high resistive zones before and after simulation. Table (5), on the other hand, represents the percent statistical analysis of the different shale volumes. It shows that the St. Error of the simulated parameters decreases remarkably. Also, it appears clear that, although the normal logging methods ignoring the clean and shaly beds in case of neutron (42%-47%) and resistivity logs (41%-48%), much more reliable values are given by the simulated data; 16% to 38% and 27% to 42% for both logs, respectively. Furthermore, the low shale volume range (56%-73%) given by the normal logging method (resistivity log) in front of the high resistive shale bed is greatly treated after the simulation to a range of 65% to 86%, which is relatively close to that given by gamma ray log (71% to 93%).

PREDICTING THE PETROPHYSICAL PARAMETERS

The for-mentioned simulation model can be used in predicting the missed sections of certain logs or even a complete run of logs in an area. It can be also used for predicating the petrophysical parameters of a proposed exploratory well providing that a satisfactory topological/geological neighbourhood constraint (hard constraint) is completely well developed in the study area.

Constraints for Simulating New Well

A number of rules and constraints must be satisfied first before going to simulate new imaginary well in a certain area. The most important of these are; 1) the well must be drilled in area with topological connected sets, 2) good correlated petrophysical parameters between wells in the same connected set and the other set in which a new well will be simulated, 3) the connected sets must attain the same structure elements and, 4) the presence of the same lithological units (entities) as interpreted from seismic sections.

The Topological Connected Sets (Connected Space)

To simulate the petrophysical parameters of a new well in certain area, we have to make sure that the set (area) of the new well is topologically connected with the other surrounding sets (areas), where many wells are already drilled and their petrophysical parameters are interpreted and well known. So we have to define the topological space and to find the relationships between the different sets in the study area based on topological/geological rules.

Topological Space (X, τ)

If we suppose that the study area is the big universe set X which consists of many small sets Di, Dj, Dk,….,Dn (Fig. 7). Then we have to check for an equivalence relationship (ρ) between the subsets to construct the topology in X. In this respect we have three properties of ρ:

Reflexive: when Di ρ Di for all i = 1,2,3,…………,n;

Symmetric: when Di ρ Dj ⇒ Dj ρ Di
for all i = 1,2,3,………...,n;

Transitive: when Di ρ Dj & Dj ρ Dk ⇒ Di ρ Dk
for all i = 1,2,3,………...,n;

The above properties between Di's and Dj's sets are achieved in case if the data of each set is reflexive to its self (normal), or symmetrical if the same results can be obtained from the relation between two sets (Di ρ Dj) by exchanging their positions (Dj ρ Di) and finally transitive if we have three sets and the relation between the first and the second (Di ρ Dj) and the relation between the second and the third (Di ρ Dk) can lead to the relation between the first and the third (Di ρ Dk).

After having the equivalence relationship between the subsets of X, then we have to construct the partitions of X as follows:

[Di] = { Dj ǀ Di ρ Dj} The cosets form the partition for X , where:

$$\bigcup_{i=1}^{n}[Di]=X \quad and \quad [Di]\bigcap[Dj]=\phi \quad for \; all \; i \neq j$$

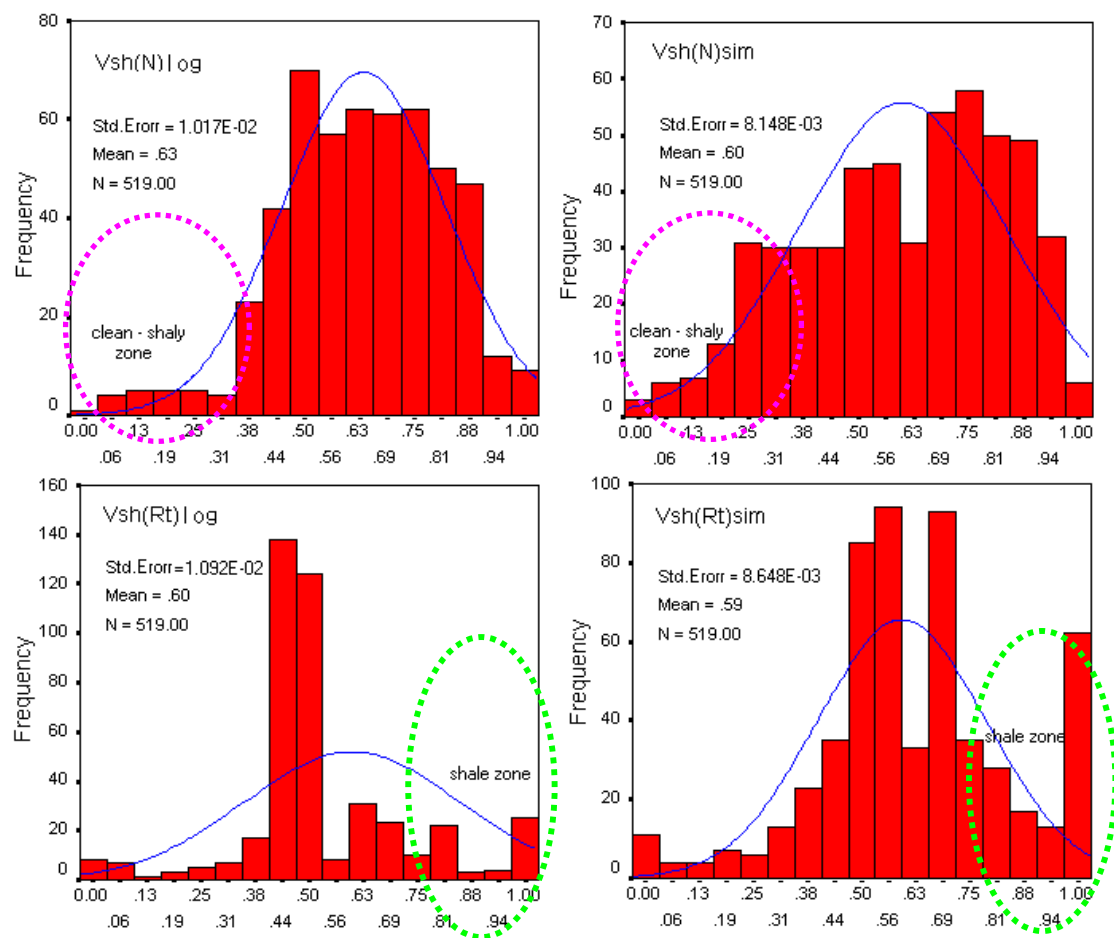These cosets construct a base for topology τ.

**Figure (6): Frequency analysis of the log estimated and the simulated
shale volumes, Nouras-1 well.**

**Table (5): Percent statistical analysis of the different shale volumes estimated using
normal logging and Monte Carlo simulation, Nouras-1 well.**

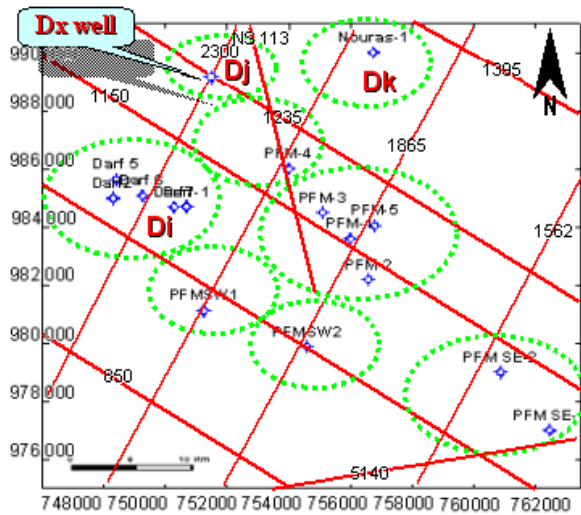|		Vsh(GR)	Vsh(Neut)sim	Vsh (Neut)log	Vsh(Rt)sim	Vsh(Rt)log
N	Valid	519	519	519	519	519
	Missing	0	0	0	0	0
Mean		.5629	.5990	.6338	.5970	.5991
Std. Error		.415E-02	8.148E-03	1.017E-02	8.648E-03	1.092E-02
Median		.5900	.6300	.6500	.5800	.5000
Variance		.1039	5.368E-02	3.446E-02	4.282E-02	6.187E-02
Range		1.00	1.00	1.00	1.00	1.00
Percentiles	10	.0030	.1600	.4200	.2700	.4100
	20	.2400	.3800	.4700	.4200	.4800
	30	.3700	.4700	.5300	.5100	.5000
	40	.5200	.5500	.5900	.5500	.5200
	50	.5900	.6300	.6500	.5800	.5400
	60	.7100	.7100	.6900	.6500	.5600
	70	.7500	.7600	.7400	.7000	.6600
	80	.9300	.8800	.8100	.8600	.7300
	90	.9900	.9200	.8600	.9000	.8300

Figure (7): Off shore Nile Delta well base map showing the seismic lines, the topological sets and location of the new well.

We have simulated many imaginary exploratory wells in the study area and we found that the best well to be drilled will be in a certain Dj set (area) according to a geological equivalence relation which can be constructed between this set and other sets (areas), for which the equivalence universal can be separated or partitioned into several areas compatible in every thing according to their petrophysical parameters (Fig. 7). We found that a good topological constraint (reflexive, symmetric and transitive relationships) is satisfied between the parameters of this area and the neighbouring Di area. Furthermore, the geological constraint is checked to choose the best location for the new exploratory well to be simulated (Fig. 8).
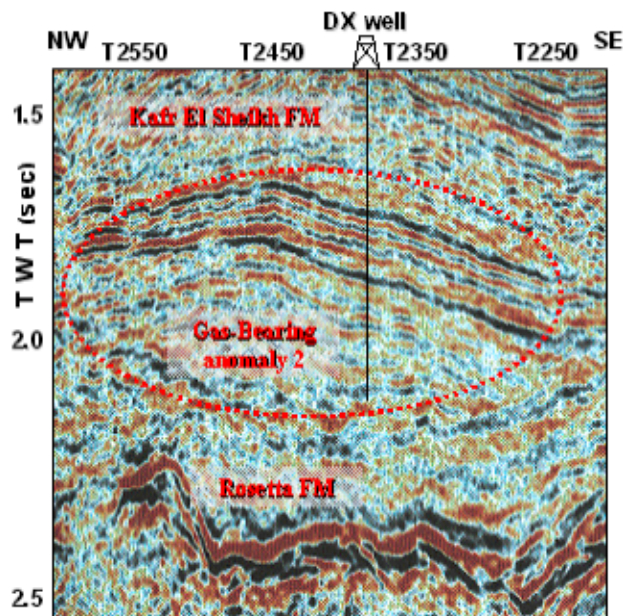

Figure (8): NW-SE seismic section (line 1235) showing the position of the new simulated well.

From lateral seismic interpretations, we have to make sure that the section to be simulated contains the same lithological entities for which the stochastic correlated parameters are already known. The new well (Dx) is chosen at the intersection of seismic lines 1235 and 2300 at shot points 2380 and 1265 for both lines, respectively. The expected two way time at the top of the gas-bearing anomaly in this well is 1.74 sec with TVD depth of -1265m. The petrophysical parameters of the well are simulated using the available datasets of the other wells in the Di set (Darfeel-1, Derfeel-2, Darfeel-7, ..etc), which have similar neighbourhood/geological characters. The following is an example of the different correlation matrices, which can be produced for a certain petrophysical property (effective porosity) of the new well by the simulation process:

$$\begin{array}{cc} & \begin{array}{ccc} \phi_{\text{eff Darf1}} & \phi_{\text{eff Darf2}} & \phi_{\text{eff Dx}} \end{array} \\ \begin{array}{c} \phi_{\text{eff Darf1}} \\ \phi_{\text{eff Darf2}} \\ \phi_{\text{eff Dx}} \end{array} & \begin{pmatrix} 1.00 & 0.95 & 0.92 \\ 0.95 & 1.00 & 0.90 \\ 0.92 & 0.90 & 1.00 \end{pmatrix} \end{array}$$

Good correlation is observed between the predicted porosity of the new well (Dx) and the simulated porosities of the other wells. The other different petrophysical parameters (Vsh, Sw, ..etc) are also simulated using the same procedure. Table (6) summarizes the average simulated petrophysical parameters of the gas-bearing anomaly-2 of the new well, relative to other wells in the study area.

Table (6): Average simulated petrophysical parameters of the gas anomaly-2 in Di and Dj sets.

Well	Zone	Vsh	Sw	φeff
Darfeel- 1	Anomaly 2	0.12	0.20	0.30
Darfeel- 2	Anomaly 2	0.17	0.35	0.25
Dx	Anomaly 2	0.21	0.46	0.27

CASE STUDY 2: RAS FANAR FIELD

Ras Fanar area is located in the central part of the western margin of the Gulf of Suez about 3.5 km east of Ras Gharib shoreline (Fig. 9). The field produces mainly from the Middle Miocene Nullipore carbonate section which is deposited under shallow marine warm water conditions and is considered to be equivalent to the Hammam Faraun Member of the Belayim Formation.

Some problems concerning with the quality of the sonic logging data are clearly noticed in this field due to the acoustic properties of the shallow carbonate section. Nullipore carbonate reservoir in Ras Fanar field is acoustically very soft especially in front of the more porous intervals (ΔT of +/- 190 μs/ft). This leads to low amplitude sonic signals and hence causes cycle skipping problems in a number of sonic logs (Fig. 10).
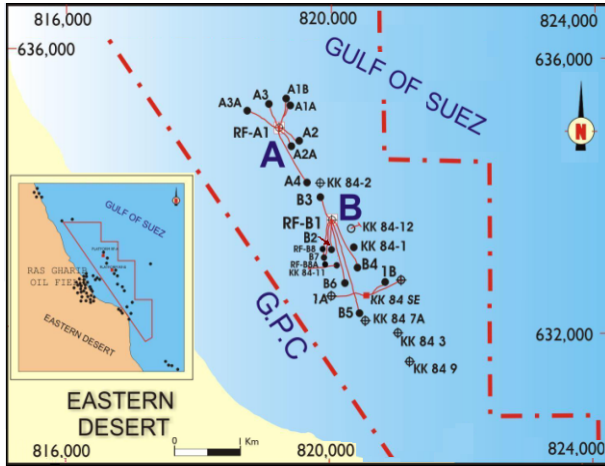
Figure (9): Well location map of Ras Fanar field.

Additionally, because the Nullipore is not well compacted (depth +/- 2000 to 3000 ftss) the usefulness of the sonic log in logging and seismic interpretations is greatly limited. With the exception of the sonic tool, almost the quality of other logs is generally good reflecting the borehole conditions.
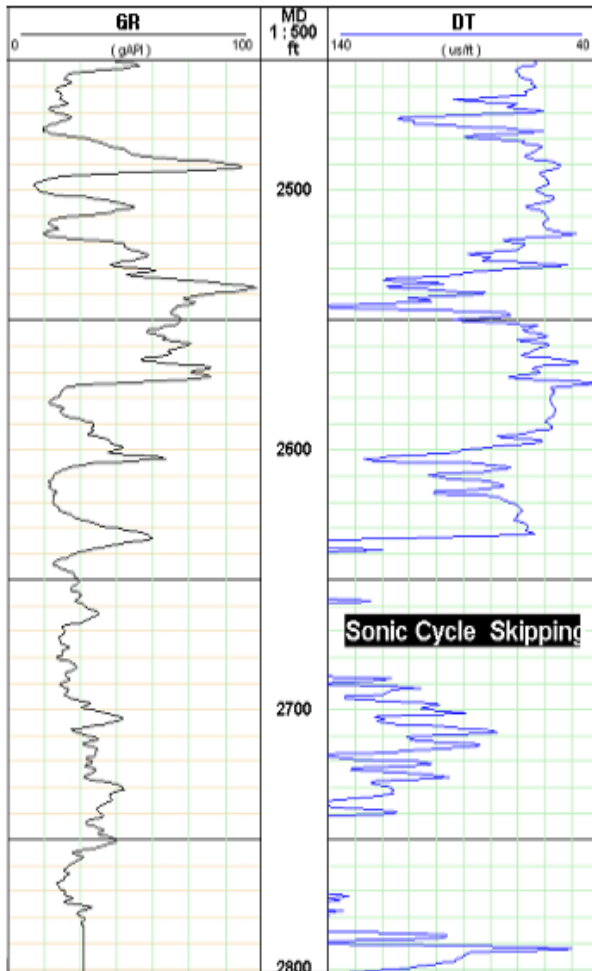

Figure (10): Cycle skipping of RF B2 well, Ras Fanar field.

To overcome cycle skipping problem and to make optimum use of the sonic log, a Monte Carlo-based simulation data are derived for sonic logs in wells where the problem exist in correlation with the other sonic data of good quality from surrounding wells. In this case study, RF B2 well is used to demonstrate how the simulation procedure could be used to enhance and improve the acoustic properties of the Nullipore carbonates. Figure (11) shows the probability density function of the sonic log for the carbonate section in RF B2 well.
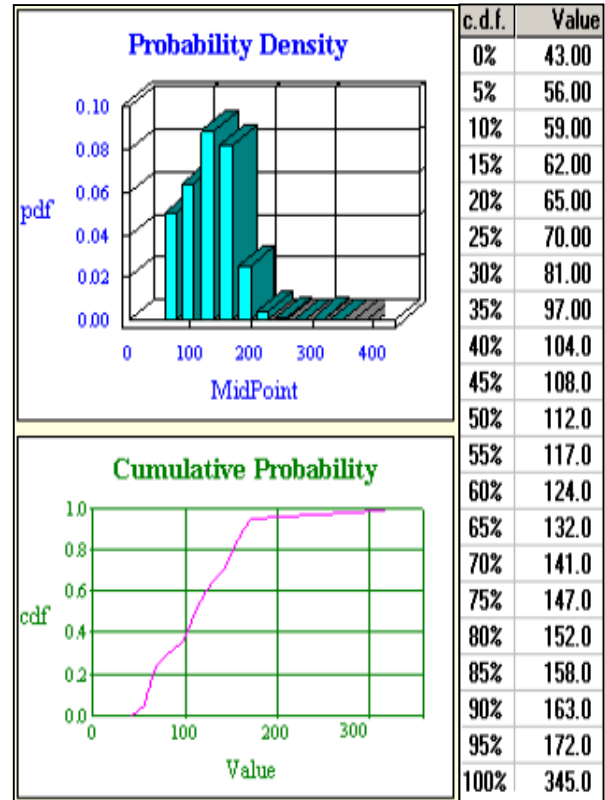

c.d.f.	Value
0%	43.00
5%	56.00
10%	59.00
15%	62.00
20%	65.00
25%	70.00
30%	81.00
35%	97.00
40%	104.0
45%	108.0
50%	112.0
55%	117.0
60%	124.0
65%	132.0
70%	141.0
75%	147.0
80%	152.0
85%	158.0
90%	163.0
95%	172.0
100%	345.0

Figure (11): Probability density function of sonic log in RF B2 well, Ras Fanar field.

It appears clear that the highest probability (best chance) for the sonic log is 0.04 with mid point of 158.9 Further more the shape of the density function assigns lognormal distribution for the simulation technique.

A Monte Carlo simulation model is applied using the parameters concluded form the probability density function and its distribution. Correlated stochastic parameters are constructed using the same procedure followed in the first case study. Much more improvements are achieved for the sonic log especially in front of the zone (2635ft-2790ft), which is greatly influenced by the cycle skipping (Fig. 12). To illustrate such enhancements, a comparison is made between the correlation matrices of the used sonic data before and after the simulation as follows:

Correlation Matrix (Logging):

$$\begin{array}{cccc} & \Delta T_{RF\,B3} & \Delta T_{RF\,B8} & \Delta T_{RF\,B2} & \Delta T_{KK\,84\text{-}1} \end{array}$$

$$\begin{array}{c} \Delta T_{RF\,B3} \\ \Delta T_{RF\,B8} \\ \Delta T_{RF\,B2} \\ \Delta T_{KK\,84\text{-}1} \end{array} \begin{pmatrix} 1.00 & 0.91 & 0.65 & 0.92 \\ 0.91 & 1.00 & 0.87 & 0.95 \\ 0.65 & 0.87 & 1.00 & 0.72 \\ 0.92 & 0.95 & 0.72 & 1.00 \end{pmatrix}$$

Correlation Matrix (MC Sim.):

$$\begin{array}{cccc} & \Delta T_{RF\,B3} & \Delta T_{RF\,B8} & \Delta T_{RF\,B2} & \Delta T_{KK\,84\text{-}1} \end{array}$$

$$\begin{array}{c} \Delta T_{RF\,B3} \\ \Delta T_{RF\,B8} \\ \Delta T_{RF\,B2} \\ \Delta T_{KK\,84\text{-}1} \end{array} \begin{pmatrix} 1.00 & 0.95 & 0.87 & 0.94 \\ 0.95 & 1.00 & 0.91 & 0.98 \\ 0.87 & 0.91 & 1.00 & 0.92 \\ 0.94 & 0.98 & 0.92 & 1.00 \end{pmatrix}$$

The correlation matrix of the simulated parameters shows that sonic log data became much correlated with other logs from the surrounding wells, especially between RF B2 well and both of RF B3 and KK 84-1 wells, where the correlation increases by percent more than 20%. Figure (12) exhibits the sonic log data of RF B2 before and after simulation.
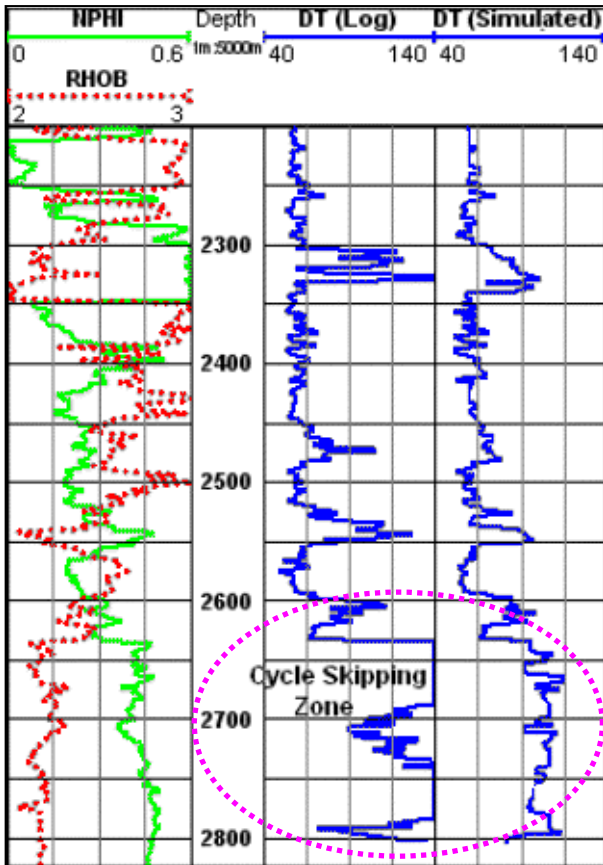

Figure (12): Sonic log data of RF B2 well before and after simulation.

SUMMARY AND CONCLUSIONS

In this study both Monte Carlo and stochastic analyses are used as powerful tools for analyzing the petrophysical parameters of the reservoirs in two different areas (offshore Nile Delta and Ras Fanar field). The purpose of these analyses is mainly to improve the estimation of the petrophysical parameters from one hand and to predict the petrophysical parameters of missed sections in old fields or even in new exploratory areas, from the other hand.

Two types of constraints are defined before going on the simulation model. The first are hard constraints based on number of probability density functions (pdf's) for the different zones, fixed petrophysical-based rules and known topological/geological relationship between the simulated wells. The second are the simulation constraints, which are matter of change and deal mainly with some stochastic realizations of the petrophysical parameters. Different types of statistical distributions and correlated multivariate variables were used in the simulation, depending on the petrophysical property to be estimated. Also, a number of correlation and variance-covariance matrices are constructed for the different logging data. The algorithm begins with simulating correlated stochastic variables one by one by running a 100 times iteration in front of each depth increment. By using rules based on the petrophysical information and by taking the best chance (most likely), much improved and new stochastically correlated petrophysical parameters, will arise.

The simulation model is used to improve the estimation of the petrophysical parameters of reservoirs, which are usually deduced by normal logging techniques. Due to the importance of shale parameters in the evaluation of the gas-bearing reservoirs in the clastic offshore succession of the Nile Delta, these parameters are chosen carefully using distributions based on Monte Carlo simulation.

Some petrophysical parameters which are not commonly used in logging interpretation due to the uncertainty (shale volume indicators) are redrawn using the simulation model. The simulated Vsh values are found more correlated and the errors in the interpretation which may arise by using normal logging techniques due to certain rock physical properties (low resistive sand and high resistive shale beds), are effectively reduced. Percent and frequency analyses are also used to compare between the results of both methods. The other important petrophysical parameters, which are necessary for evaluating the studied reservoirs, are all simulated and estimated using suitable Monte Carlo distributions.

Furthermore, the model is used to predicate the petrophysical parameters of a new proposed well (Dx) in the offshore Nile Delta. To do that, the main area (X) is subdivided topologically into small areas (sets) Di, Dj, Dk,….,Dn and a hard topological/geological neighbourhood constraint is examined first. An equivalence relationship (ρ) between the subsets is studied to find the topological properties (reflexive, symmetric and transitive) of the different sets based on geological/petrophysical rules. The different petrophysical parameters of the new well (ϕ, Vsh, Sw, ..etc) are all simulated and predicted.

In Ras Fanar field, on the other hand, the model is used to solve the cycle skipping problem concerning with sonic log, which is a common phenomenon in this field due to the acoustic properties of the carbonate Nullipore reservoir. The quality of the simulated sonic data are greatly improved and show much more correlation with other sonic data of good quality ($\rho > 87\%$).

The interpretations and results obtained form the simulation model are proved to be more accurate and representative for the petrophysical properties of the studied reservoirs than that obtained form normal logging analyses. So, this simulation model has a wide range of applicability and can be either used to improve the estimation of the petrophysical parameters of the reservoirs and/or to make optimum use of the available data in old fields or even in to predict the petrophysical parameters of wells in new exploratory areas.

REFERENCES

Alabert, F. G., and Massonnat, G. J., (1990): Heterogeneity in a complex turbiditic reservoir: Stochastic modeling of facies and petrophysical variability. Society of Petroleum Engineers Annual Technical Conference and Exhibition, New Orleans, Louisiana, pp: 776- 790.

Bartlett, M. S. (1966): An introduction to stochastic processes, 2nd ed. Cambridge University Press, Cambridge.

Bortoli, L. J., Alabert, F. G., Haas, A. G., and Journal, A. G., (1993): Constraining stochastic images to seismic data, in Geostatistics Troia 92, 1, edited by Soares, A., Kluwer. Academic Publishers, Dodrecht, Netherlands, pp: 325-337.

de Groot, P. F. M., Bril, A. H., Florist, F. J. T., and Campbell, A. E., (1996): Monte Carlo simulation of wells. Geophysics, V. 61, No.3, pp: 631-638.

de Groot, P. F. M., Campbell, A. E., and Kavli, T., (1993): Seismic reservoir characterization using artificial neural networks and stochastic modelling techniques: 55th Conf. Eur. Assn. Expl. Geophys., Stavanger, Expanded Abstracts, paper B047.

Deutsch, C. V., (2002): Geostatistical reservoir modelling. New York, Oxford University Press, 376p.

Fogg, G. E., Lucia, J. F., and Senger, R. K., (1991): Stochastic simulation of interwell scale heterogeneity for improved prediction of sweep efficiency in a carbonate reservoir, in Reservoir Characterization II, edited by Lake, L. W., Carroll, H. B., Jr., and Wesson, T. C., Academic Press Inc., Orlando, Florida, pp: 487-544.

Haldorsen, H. H., and Chang, D. W., (1986): Notes on stochastic shales; from outcrop to simulation model, in L. W. Lake and H. B. Caroll, eds., Reservoir characterization: London, Academic Press, pp: 445- 48.

Haldorsen, H. H., and Damsleth, E., (1990): Stochastic modelling. Journal of Petroleum Technology, V. 42, No. 4, pp: 404-412.

Hearst, J. R, and Nelson, P. H., (1985): Well logging for physical properties. McGraw-Hill, N. Y., 189p.

Isaaks, E. H., and Srivastava, R. M., (1989): An introduction to applied geostatistics. Oxford University Press, New York, 561p.

Law, A. M., and Kelton, W. D., (1991): Simulation modeling & Analysis. 2nd ed. New York, McGraw Hill, Inc.

Molz, F. J., and Boman, G. K., (1993): A fractal-based stochastic interpolation scheme in subsurface hydrology. Water Resour. Res., V. 29, No.11, pp: 3769-3774.

Pyrcz, M. J., Catuneanu , O., and Deutsch, C. V., (2005): Stochastic surface-based modelling of turbidite lobes. AAPG Bulletin, V. 89, No. 2, pp: 177-191

Pyrcz, M. J., and Deutsch, C. V., (2003): Stochastic surface modelling in mud rich, fine-grained turbidite lobes (abs.). AAPG Annual Meeting, May 11–14, Salt Lake City, Utah, Extended abstract, 6p.

Rubinstein, R. Y. (1981): Simulation and the Monte Carlo method. New York, John Wiley & Sons.

Sambridge, M., and Mosegaard, K., (2002): Monte Carlo methods in geophysical inverse problems. American Geophysical Union. Reviews of Geophysics, V. 40, No. 3, 29p.

Schlumberger Charts, (1991): Log interpretation charts. Schlumberger Educational Services. Houston, Texas, U.S.A, 171p.

Strauss D. J., and Sadler, P. M., (1989): Stochastic models for the completeness of stratigraphic sections. Math. Geol., 21, pp: 37-59.